

Synthesis, Photophysics, and Electrochemistry of Luminescent Binuclear Rhenium(I) Complexes Containing μ -Bridging Thiolates. X-ray Crystal Structure of $[\{\text{Re}(\text{bpy})(\text{CO})_3\}_2(\mu\text{-SC}_6\text{H}_4\text{-CH}_3\text{-}p)\text{]OTf}$

Vivian Wing-Wah Yam,* Keith Man-Chung Wong, and Kung-Kai Cheung

Department of Chemistry, The University of Hong Kong, Pokfulam Road, Hong Kong

Received September 17, 1996[®]

A series of binuclear Re(I) thiolato complexes $[\{\text{Re}(\text{L-L})(\text{CO})_3\}_2(\mu\text{-SC}_6\text{H}_4\text{-X-}p)\text{]OTf}$ [L-L = phen, X = CH₃ (**1**), OCH₃ (**2**), C(CH₃)₃ (**3**), Cl (**4**), F (**5**); L-L = bpy, X = CH₃ (**6**); L-L = 5,5'-Me₂-bpy, X = CH₃ (**7**)] have been synthesized and their photophysical and electrochemical properties studied. The X-ray crystal structure of **6** has also been determined. The complexes have been shown to exhibit long-lived luminescence both in the solid state and in fluid solutions at room temperature. The emission has been assigned as being derived from a ³MLCT origin.

Introduction

Rhenium(I) tricarbonyl α,α' -diimine systems have been extensively studied for their rich photoluminescent properties and their ability to effect electrocatalytic reduction of carbon dioxide. Numerous reports on the photophysical and photochemical studies have appeared as a result of the sensitivity of their luminescent behavior to changes in the nature of the environment as well as their stability to photodecomposition.^{1–5} The electrocatalytic reduction of carbon dioxide employing such a system has also been widely studied by bulk electrolysis, cyclic voltammetry, and IR spectroelectrochemical investigations.⁶

Recently, there has been a growing interest in the studies of rhenium–sulfur complexes owing to their possible involvement in hydrodesulfurization catalysis.⁷

Besides, the well-documented MLCT excited state chemistry of rhenium(I) α,α' -diimine complexes,^{1–5} together with our recent interest in the photophysical studies of polynuclear metal–chalcogen systems,⁸ has attracted our attention to the synthesis of luminescent complexes of rhenium(I) thiolates. Thiolate ligands are also well-known to have different bonding modes, capable of forming polynuclear complexes with various transition metal ions.⁹ To the best of our knowledge, there have been no reports on the photophysical studies of rhenium(I)–thiolato complexes despite a number of rhenium thiolate systems, limited to those of structural studies, being known.¹⁰ Moreover, despite numerous studies on supramolecular chemistry employing bridging diimine ligands,^{1b,3a,4c,11} attempts to utilize the ability of the thiolate ligand to bridge various metal centers in the design of supramolecular systems were not known. Therefore, it is our aim to employ thiolate ligands in the synthesis and design of polynuclear luminescent rhenium(I) tricarbonyl α,α' -diimine complexes and to fine tune their excited state behavior through the systematic variation of the thiolate ligand. In this work, we report the synthesis, photophysics, and electrochemistry of a series of luminescent binuclear rhenium(I) complexes containing μ -bridging thiolato

[®] Abstract published in *Advance ACS Abstracts*, March 15, 1997.

(1) See, for example: (a) Horváth, O.; Stevenson, K. L. *Charge Transfer Photochemistry of Coordination Compounds*; VCH: New York, 1993. (b) Balzani, V.; Scandola, F. *Supramolecular Photochemistry*; Ellis Horwood: Chichester, U.K., 1991.

(2) See, for example: (a) Wrighton, M. S.; Morse, D. L. *J. Am. Chem. Soc.* **1974**, *96*, 998. (b) Wrighton, M. S. *J. Am. Chem. Soc.* **1974**, *74*, 4801. (c) Fredericks, S. M.; Luong, J. C.; Wrighton, M. S. *J. Am. Chem. Soc.* **1979**, *101*, 7415.

(3) See, for example: (a) Wallendaal, S. V.; Shaver, R. J.; Rillema, D. P.; Yoblinski, B. J.; Stathis, M.; Guarr, T. F. *Inorg. Chem.* **1990**, *29*, 1761. (b) Sacksteder, L. A.; Zipp, A. P.; Brown, E. A.; Streich, J.; Demas, J. N.; DeGraff, B. A. *Inorg. Chem.* **1990**, *29*, 4335. (c) Sacksteder, L. A.; Lee, M.; Demas, J. N.; DeGraff, B. A. *J. Am. Chem. Soc.* **1993**, *115*, 8230. (d) Wallace, L.; Woods, C.; Rillema, D. P. *Inorg. Chem.* **1995**, *34*, 2875. (e) Stufkens, D. J. *Comments Inorg. Chem.* **1992**, *13*, 359. (f) Sullivan, B. P. *J. Phys. Chem.* **1989**, *93*, 24. (g) Lees, A. J. *Chem. Rev.* **1987**, *87*, 711.

(4) See, for example: (a) Caspar, J. V.; Meyer, T. J. *J. Phys. Chem.* **1983**, *87*, 952. (b) Tapolsky, G. T.; Duesing, R.; Meyer, T. J. *J. Phys. Chem.* **1989**, *93*, 3885. (c) Tapolsky, G. T.; Duesing, R.; Meyer, T. J. *Inorg. Chem.* **1990**, *29*, 2285.

(5) See, for example: (a) Yam, V. W.-W.; Lau, V. C.-Y.; Cheung, K.-K. *J. Chem. Soc., Chem. Commun.* **1995**, 259. (b) Yam, V. W.-W.; Lau, V. C.-Y.; Cheung, K.-K. *Organometallics* **1995**, *14*, 2749. (c) Yam, V. W.-W.; Lau, V. C.-Y.; Cheung, K.-K. *Organometallics* **1996**, *15*, 1740. (d) Yam, V. W.-W.; Wong, K. M.-C.; Lee, V. W.-M.; Lo, K. K.-W.; Cheung, K.-K. *Organometallics* **1995**, *14*, 4034.

(6) See, for example: (a) Hawecker, J.; Lehn, J. M.; Ziessel, R. *J. Chem. Soc., Chem. Commun.* **1984**, 328. (b) Sullivan, B. P.; Meyer, T. J. *J. Chem. Soc., Chem. Commun.* **1984**, 1244. (c) Sullivan, B. P.; Bolinger, C. M.; Conrad, D.; Vining, W. J.; Meyer, T. J. *J. Chem. Soc., Chem. Commun.* **1985**, 1414. (d) Breikss, A. I.; Abruna, H. D. *J. Electroanal. Chem.* **1986**, *201*, 347. (e) Luong, J. C. Ph.D. Thesis, Massachusetts Institute of Technology, Cambridge, MA, 1981.

(7) See, for example: (a) Pecoraro, T. A.; Chianelli, R. R. *J. Catal.* **1981**, *67*, 430. (b) Ledoux, M. J.; Michaux, O.; Agostini, G.; Panissod, P. *J. Catal.* **1986**, *102*, 275. (c) Bussell, M. E.; Somorjai, G. A. *J. Phys. Chem.* **1989**, *93*, 2009.

(8) See, for example: (a) Yam, V. W.-W.; Lee, W.-K.; Lai, T.-F. *J. Chem. Soc., Chem. Commun.* **1993**, 1571. (b) Yam, V. W.-W.; Yeung, P. K.-Y.; Cheung, K.-K. *J. Chem. Soc., Chem. Commun.* **1995**, 256. (c) Yam, V. W.-W.; Yeung, P. K.-Y.; Cheung, K.-K. *J. Chem. Soc., Dalton Trans.* **1994**, 12, 2197. (d) Yam, V. W.-W.; Lo, K. K.-W.; Cheung, K. K. *Inorg. Chem.* **1996**, *35*, 3459. (e) Yam, V. W.-W.; Lo, K. K.-W.; Wang, C.-R.; Cheung, K. K. *Inorg. Chem.* **1996**, *35*, 5116. (f) Yam, V. W.-W.; Yeung, P. K.-Y.; Cheung, K.-K. *Angew. Chem., Int. Ed. Engl.* **1996**, *35*, 739. (g) Yam, V. W.-W.; Chan, C.-L.; Cheung, K.-K. *J. Chem. Soc., Dalton Trans.* **1996**, 4019.

(9) Krebs, B.; Henkel, G. *Angew. Chem., Int. Ed. Engl.* **1991**, *30*, 769.

(10) See, for example: (a) Osborne, A. G.; Stone, F. G. A. *J. Chem. Soc. A* **1969**, 1143. (b) King, R. B.; Welcman, N. *Inorg. Chem.* **1969**, *12*, 2540. (c) Abel, E. W.; Harrison, W.; McLean, R. A. N.; Marsh, W. C.; Trotter, J. *J. Chem. Soc., Chem. Commun.* **1970**, 1531.

(11) See, for example: (a) Volger, A.; Kisslinger, J. *Inorg. Chim. Acta* **1986**, *115*, 119. (b) Juris, A.; Campagna, S. Bidd, I.; Lehn, J. M.; Ziessel, R. *Inorg. Chem.* **1988**, *27*, 4007.

ligands. The crystal structure of $[\{\text{Re}(\text{bpy})(\text{CO})_3\}_2(\mu\text{-SC}_6\text{H}_4\text{-CH}_3\text{-}p)]\text{OTf}$ has also been determined.

Experimental Section

Materials and Reagents. $[\text{Re}(\text{CO})_5\text{Cl}]$ was obtained from Strem Chemicals, Inc. 1,10-Phenanthroline (phen) and 2,2'-bipyridine (bpy) were obtained from Aldrich Chemical Co. 5,5'-Dimethyl-2,2'-bipyridine ($\text{Me}_2\text{-bpy}$) was prepared by the slight modification of a reported procedure.¹² *p*-Thiocresol, 4-*tert*-butylthiophenol, 4-methoxythiophenol, and 4-chlorothiophenol were obtained from Lancaster Synthesis Ltd. 4-Fluorothiophenol was purchased from Aldrich Chemical Co. Both acetonitrile and dichloromethane were distilled over calcium hydride before use. Tetrahydrofuran was distilled over sodium benzophenone ketyl before use. All other reagents and solvents were of analytical grade and were used as received. $[\text{Re}(\text{L}-\text{L})(\text{CO})_3(\text{MeCN})]\text{OTf}$ (L-L = phen, bpy, or $\text{Me}_2\text{-bpy}$) were prepared according to literature procedures.^{2c}

Syntheses of Rhenium Complexes. All reactions were performed under anaerobic and anhydrous conditions using standard Schlenk technique under an inert atmosphere of nitrogen.

$[\{\text{Re}(\text{phen})(\text{CO})_3\}_2(\mu\text{-SC}_6\text{H}_4\text{-CH}_3\text{-}p)]\text{OTf}$ (1). To a stirred suspension of $[\text{Re}(\text{phen})(\text{CO})_3(\text{MeCN})]\text{OTf}$ (100 mg, 0.16 mmol) in THF (20 mL) was added a solution of $\text{Et}_3\text{NHSC}_6\text{H}_4\text{-CH}_3\text{-}p$ (0.10 mmol) in THF (10 mL), prepared *in situ* from $\text{HSC}_6\text{H}_4\text{-CH}_3\text{-}p$ (12.4 mg, 0.10 mmol) and excess Et_3N , under an inert atmosphere of nitrogen. The reaction mixture was stirred for 48 h, after which the solvent was removed under vacuum. The product was then purified by column chromatography on silica gel using dichloromethane-acetone (9:1 v/v) as eluent. The first band gave the monomeric $[\text{Re}(\text{phen})(\text{CO})_3(\text{SC}_6\text{H}_4\text{-CH}_3\text{-}p)]$, while the second band gave the desired product. Recrystallization by slow vapor diffusion of diethyl ether into an acetone solution of the complex gave **1** as yellow crystals. Yield: 122 mg, 65%. ¹H NMR (300 MHz, acetone-*d*₆, 298 K, relative to TMS): δ 1.85 (s, 3H, Me), 4.95 (dd, 2H, aryl H *ortho* to S), 5.75 (dd, 2H, aryl H *meta* to S), 7.70 (dd, 4H, phen H's), 7.90 (s, 4H, phen H's), 8.50 (dd, 4H, phen H's), 8.90 (dd, 4H, phen H's). IR (CH₂Cl₂, cm⁻¹): $\nu(\text{C}=\text{O})$ 2033, 2022, 1929, 1916. Positive FAB-MS: ion clusters at m/z 1025 $\{\text{M}\}^+$, 993 $\{\text{M} - \text{CO}\}^+$, 574 $\{\text{M} - [\text{Re}(\text{phen})(\text{CO})_3]\}^+$, 451 $\{\text{M} - [\text{Re}(\text{phen})(\text{CO})_3(\text{SC}_6\text{H}_4\text{-CH}_3\text{-}p)]\}^+$. UV-vis [λ/nm ($\epsilon_{\text{max}}/\text{dm}^3 \text{mol}^{-1} \text{cm}^{-1}$): CH₂Cl₂, 270 (49 670), 290 sh (30 765), 370 (7425), 440 sh (2620). Elemental analyses. Found: C, 38.98; H, 1.86; N, 4.50. Calcd for **1**: C, 38.89; H, 1.96; N, 4.78.

$[\{\text{Re}(\text{phen})(\text{CO})_3\}_2(\mu\text{-SC}_6\text{H}_4\text{-OCH}_3\text{-}p)]\text{OTf}$ (2). The procedure is similar to that described for the preparation of **1**, except 4-methoxythiophenol was used in place of *p*-thiocresol to give yellow crystals of **2**. Yield: 124 mg, 65%. ¹H NMR (300 MHz, acetone-*d*₆, 298 K, relative to TMS): δ 3.45 (s, 3H, *OMe*), 4.90 (dd, 2H, aryl H *ortho* to S), 5.40 (dd, 2H, aryl H *meta* to S), 7.95 (dd, 4H, phen H's), 8.05 (s, 4H, phen H's), 8.75 (dd, 4H, phen H's), 9.25 (dd, 4H, phen H's). IR (CH₂Cl₂, cm⁻¹): $\nu(\text{C}=\text{O})$ 2033, 2022, 1929, 1915. Positive FAB-MS: ion clusters at m/z 1041 $\{\text{M}\}^+$, 590 $\{\text{M} - [\text{Re}(\text{phen})(\text{CO})_3]\}^+$, 451 $\{\text{M} - [\text{Re}(\text{phen})(\text{CO})_3(\text{SC}_6\text{H}_4\text{-OCH}_3\text{-}p)]\}^+$. UV-vis [λ/nm ($\epsilon_{\text{max}}/\text{dm}^3 \text{mol}^{-1} \text{cm}^{-1}$): CH₂Cl₂, 278 (4300), 286 sh (29 180), 364 (8180), 434 sh (3315). Elemental analyses. Found: C, 38.91; H, 1.70; N, 4.73. Calcd for **2**: C, 38.56; H, 2.04; N, 4.67.

$[\{\text{Re}(\text{phen})(\text{CO})_3\}_2(\mu\text{-SC}_6\text{H}_4\text{-C}(\text{CH}_3)_3\text{-}p)]\text{OTf}$ (3). The procedure is similar to that described for the preparation of **1**, except 4-*tert*-butylthiophenol was used in place of *p*-thiocresol to give yellow crystals of **3**. Yield: 126 mg, 65%. ¹H NMR (300 MHz, acetone-*d*₆, 298 K, relative to TMS): δ 1.10 (s, 9H, ^tBu), 5.00 (dd, 2H, aryl H *ortho* to S), 5.95 (dd, 2H, aryl H *meta* to S), 8.10 (dd, 4H, phen H's), 8.15 (s, 4H, phen H's),

8.90 (dd, 4H, phen H's), 9.45 (dd, 4H, phen H's). IR (CH₂Cl₂, cm⁻¹): $\nu(\text{C}=\text{O})$ 2033, 2021, 1931, 1915. Positive FAB-MS: ion clusters at m/z 1065 $\{\text{M}\}^+$, 616 $\{\text{M} - [\text{Re}(\text{phen})(\text{CO})_3]\}^+$, 451 $\{\text{M} - [\text{Re}(\text{phen})(\text{CO})_3(\text{SC}_6\text{H}_4\text{-}^t\text{Bu-}p)]\}^+$. UV-vis [λ/nm ($\epsilon_{\text{max}}/\text{dm}^3 \text{mol}^{-1} \text{cm}^{-1}$): CH₂Cl₂, 270 (41 345), 294 sh (23 630), 366 (6905), 438 sh (2280). Elemental analyses. Found: C, 41.12; H, 2.21; N, 4.59. Calcd for **3**: C, 41.02; H, 2.57; N 4.50.

$[\{\text{Re}(\text{phen})(\text{CO})_3\}_2(\mu\text{-SC}_6\text{H}_4\text{-Cl-}p)]\text{OTf}$ (4). The procedure is similar to that described for the preparation of **1**, except 4-chlorothiophenol was used in place of *p*-thiocresol to give yellow crystals of **4**. Yield: 123 mg, 65%. ¹H NMR (300 MHz, acetone-*d*₆, 298 K, relative to TMS): δ 5.15 (dd, 2H, aryl H *ortho* to S), 5.75 (dd, 2H, aryl H *meta* to S), 7.95 (dd, 4H, phen H's), 8.10 (s, 4H, phen H's), 8.80 (dd, 4H, phen H's), 9.25 (dd, 4H, phen H's). IR (CH₂Cl₂, cm⁻¹): $\nu(\text{C}=\text{O})$ 2034, 2024, 1932, 1914. Positive FAB-MS: ion clusters at m/z 1029 $\{\text{M}\}^+$, 594 $\{\text{M} - [\text{Re}(\text{phen})(\text{CO})_3]\}^+$, 451 $\{\text{M} - [\text{Re}(\text{phen})(\text{CO})_3(\text{SC}_6\text{H}_4\text{-Cl-}p)]\}^+$. UV-vis [λ/nm ($\epsilon_{\text{max}}/\text{dm}^3 \text{mol}^{-1} \text{cm}^{-1}$): CH₂Cl₂, 278 (41 590), 286 sh (28 900), 366 (7700), 436 sh (2825). Elemental analyses. Found: C, 37.69; H, 1.50; N, 4.70. Calcd for **4**: C, 37.52; H, 1.78; N, 4.64.

$[\{\text{Re}(\text{phen})(\text{CO})_3\}_2(\mu\text{-SC}_6\text{H}_4\text{-F-}p)]\text{OTf}$ (5). The procedure is similar to that described for the preparation of **1**, except 4-fluorothiophenol was used in place of *p*-thiocresol to give yellow crystals of **5**. Yield: 124 mg, 65%. ¹H NMR (300 MHz, acetone-*d*₆, 298 K, relative to TMS): δ 5.10 (dd, 2H, aryl H *ortho* to S), 5.90 (dd, 2H, aryl H *meta* to S), 7.75 (dd, 4H, phen H's), 7.95 (s, 4H, phen H's), 8.50 (dd, 4H, phen H's), 8.95 (dd, 4H, phen H's). IR (CH₂Cl₂, cm⁻¹): $\nu(\text{C}=\text{O})$ 2034, 2023, 1937, 1915. Positive FAB-MS: ion clusters at m/z 1045 $\{\text{M}\}^+$, 594 $\{\text{M} - [\text{Re}(\text{phen})(\text{CO})_3]\}^+$. UV-vis [λ/nm ($\epsilon_{\text{max}}/\text{dm}^3 \text{mol}^{-1} \text{cm}^{-1}$): CH₂Cl₂, 272 (44 810), 294 sh (26 520), 366 (7525), 440 sh (2975). Elemental analyses. Found: C, 38.44; H, 1.44; N, 4.76. Calcd for **5**: C, 38.04; H, 1.81; N, 4.70.

$[\{\text{Re}(\text{bpy})(\text{CO})_3\}_2(\mu\text{-SC}_6\text{H}_4\text{-CH}_3\text{-}p)]\text{OTf}$ (6). The procedure is similar to that described for the preparation of **1**, except $[\text{Re}(\text{bpy})(\text{CO})_3(\text{MeCN})]\text{OTf}$ was used in place of $[\text{Re}(\text{phen})(\text{CO})_3(\text{MeCN})]\text{OTf}$ to give yellow crystals of **6**. Yield: 117 mg, 70%. ¹H NMR (300 MHz, CDCl₃, 298 K, relative to TMS): δ 2.10 (s, 3H, Me), 5.90 (dd, 2H, aryl H *ortho* to S), 6.35 (dd, 2H, aryl H *meta* to S), 7.25 (m, 4H, bpy H's), 8.05 (dd, 4H, bpy H's), 8.20 (dd, 4H, bpy H's), 8.50 (dd, 4H, bpy H's). IR (CH₂Cl₂, cm⁻¹): $\nu(\text{C}=\text{O})$ 2033, 2022, 1927, 1915. Positive FAB-MS: ion clusters at m/z 975 $\{\text{M}\}^+$, 550 $\{\text{M} - [\text{Re}(\text{bpy})(\text{CO})_3]\}^+$, 427 $\{\text{M} - [\text{Re}(\text{bpy})(\text{CO})_3(\text{SC}_6\text{H}_4\text{-CH}_3\text{-}p)]\}^+$. UV-vis [λ/nm ($\epsilon_{\text{max}}/\text{dm}^3 \text{mol}^{-1} \text{cm}^{-1}$): CH₂Cl₂, 290 (20 730), 310 sh (15 305), 368 (5590), 438 sh (2700). Elemental analyses. Found: C, 36.47; H, 1.95; N, 4.94. Calcd for **6**: C, 36.29; H, 2.05; N, 4.98.

$[\{\text{Re}(\text{Me}_2\text{-bpy})(\text{CO})_3\}_2(\mu\text{-SC}_6\text{H}_4\text{-CH}_3\text{-}p)]\text{OTf}$ (7). The procedure is similar to that described for the preparation of **1**, except $[\text{Re}(\text{Me}_2\text{-bpy})(\text{CO})_3(\text{MeCN})]\text{OTf}$ was used in place of $[\text{Re}(\text{bpy})(\text{CO})_3(\text{MeCN})]\text{OTf}$ to give yellow crystals of **7**. Yield: 122 mg, 65%. ¹H NMR (300 MHz, acetone-*d*₆, 298 K, relative to TMS): δ 2.15 (s, 3H, methyl H's *para* to S), 2.40 (s, 12H, methyl H's on $\text{Me}_2\text{-bpy}$), 6.00 (d, 2H, aryl H *ortho* to S), 6.45 (d, 2H, aryl H *meta* to S), 7.95 (d, 4H, $\text{Me}_2\text{-bpy}$ H's), 8.25 (d, 4H, $\text{Me}_2\text{-bpy}$ H's), 8.50 (s, 4H, $\text{Me}_2\text{-bpy}$ H's), 9.25 (dd, 4H, $\text{Me}_2\text{-bpy}$ H's). IR (CH₂Cl₂, cm⁻¹): $\nu(\text{C}=\text{O})$ 2030, 2020, 1922, 1913. Positive FAB-MS: ion clusters at m/z 1026 $\{\text{M}\}^+$, 575 $\{\text{M} - [\text{Re}(\text{Me}_2\text{-bpy})(\text{CO})_3]\}^+$, 453 $\{\text{M} - [\text{Re}(\text{Me}_2\text{-bpy})(\text{CO})_3(\text{SC}_6\text{H}_4\text{-CH}_3\text{-}p)]\}^+$. UV-vis [λ/nm ($\epsilon_{\text{max}}/\text{dm}^3 \text{mol}^{-1} \text{cm}^{-1}$): CH₂Cl₂, 316 (37 515), 328 sh (32 410), 374 (6375), 422 sh (4120). Elemental analyses. Found: C, 38.45; H, 2.75; N, 4.56. Calcd for **7**: C, 38.63; H, 2.63; N, 4.74.

Physical Measurements and Instrumentation. UV-visible spectra were obtained on a Hewlett-Packard 8452A diode array spectrophotometer, IR spectra on a Bio-Rad FTS-7 Fourier transform infrared spectrophotometer (4000–400 cm⁻¹), and steady state excitation and emission spectra on a Spex Fluorolog 111 spectrofluorometer equipped with a Hamamatsu R-928 photomultiplier tube. Low-temperature (77 K) spectra were recorded by using an optical Dewar quartz

(12) Sprintschnik, G.; Sprintschnik, H. W.; Whitten, D. G. *J. Am. Chem. Soc.* **1977**, *99*, 4947.

Table 1. Crystal and Structure Determination Data for 6

formula	Re ₂ SO ₆ N ₄ C ₃₃ H ₂₃ ⁺ CF ₃ SO ₃ ⁻
fw	1125.11
T, K	301
a, Å	10.488(2)
b, Å	18.599(4)
c, Å	10.173(2)
α, deg	91.60(2)
β, deg	100.21(2)
γ, deg	73.98(1)
V, Å ³	1876.7(6)
crystal color and shape	yellow prism
crystal system	triclinic
space group	P $\bar{1}$
Z	2
F(000)	1072
D _c , g cm ⁻³	1.991
crystal dimensions, mm	0.30 × 0.25 × 0.25
λ, Å (graphite monochromated, Mo Kα)	0.710 73
μ, cm ⁻¹	66.31
collection range	2θ _{max} = 48° (h, 0–11; k, –20 to 20; l, –11 to 11)
scan mode and scan speed, deg min ⁻¹	ω–2θ, 16.0
scan width, deg	0.79 + 0.35 tan θ
no. of data collected	6263
no. of unique data	5893
no. of data used in refinement, m	4950
no. of parameters refined, p	488
R ^a	0.029
wR ^a	0.039
goodness-of fit, S	1.74
maximum shift, (Δ/σ) _{max}	0.03
residual extremes in final difference map, e Å ⁻³	+1.60, –1.07

^a $w = 4F_o^2/\sigma^2(F_o^2)$, where $\sigma^2(F_o^2) = [\sigma^2(I) + (0.028 F_o^2)^2]$ with $I \geq 3\sigma(I)$.

sample holder. ¹H NMR spectra were recorded on a Bruker DPX 300 Fourier transform NMR spectrometer with chemical shifts reported relative to tetramethylsilane. Positive ion FAB mass spectra were recorded on a Finnigan MAT95 mass spectrometer. Elemental analyses of the new complexes were performed by Butterworth Laboratories Ltd.

Cyclic voltammetric measurements were performed by using a CH Instruments, Inc. Model CHI 620 electrochemical analyzer interfaced to an IBM-compatible 486 personal computer. The electrolytic cell used was a conventional two-compartment cell. The salt bridge of the reference electrode was separated from the working electrode compartment by a Vycor glass. A Ag/AgNO₃ (0.1 mol dm⁻³ in CH₃CN) reference electrode was used. The ferrocenium–ferrocene couple was used as the internal standard in the electrochemical measurements in acetonitrile (0.1 mol dm⁻³ NBu₄PF₆).^{13a} The working electrode was a glassy carbon (Atomergic Chemetals V25) electrode with a platinum foil acting as the counter electrode. Treatment of the electrode surfaces was as reported previously.^{13b}

Emission lifetime measurements were performed using a conventional laser system. The excitation source was the 355-nm output (third harmonic) of a Quanta-Ray Q-switched GCR-150-10 pulsed Nd–YAG laser. Luminescence decay signals were recorded on a Tektronix Model TDS-620A (500 MHz, 2 GS/s) digital oscilloscope and analyzed using a program for exponential fits. All solutions for photophysical studies were prepared under vacuum in a 10-cm³ round-bottom flask equipped with a side arm 1-cm fluorescence cuvette and sealed from the atmosphere by a Kontes quick-release Teflon stopper. Solutions were rigorously degassed with no fewer than four freeze–pump–thaw cycles. Luminescence quantum yields, Φ_{em}, were measured at room temperature by the Parker-Rees method using [Ru(bpy)₃]²⁺ as a standard.¹⁴

Crystal Structure Determination. Crystals of **6** were obtained by slow diffusion of diethyl ether into an acetone

solution of the complex. *Crystal Data.* {[Re₂SO₆N₄C₃₃H₂₃]⁺CF₃SO₃⁻}; M_r = 1125.11, triclinic, space group P $\bar{1}$ (No. 2), a = 10.488(2) Å, b = 18.599(4) Å, c = 10.173(2) Å, α = 91.60(2)°, β = 100.21(2)°, γ = 73.98(1)°, V = 1876.7(6) Å³, Z = 2, D_c = 1.991 g cm⁻³, μ(Mo Kα) = 66.31 cm⁻¹, F(000) = 1072, T = 301 K. A yellow crystal of dimensions 0.30 × 0.25 × 0.25 mm was used for data collection at 28 °C on a Rigaku AFC7R diffractometer with graphite monochromatized Mo Kα radiation (λ = 0.710 73 Å) using ω–2θ scans with ω-scan angle (0.73 + 0.35 tan θ)° at a scan speed of 16.0 deg min⁻¹ (up to six scans for reflection I < 15σ(I)). Intensity data (in the range of 2θ_{max} = 48°; h, 0–11; k, –20 to 20; l, –11 to 11 and 3 standard reflections measured after every 300 reflections showed no decay) were corrected for Lorentz and polarization effects and empirical absorption corrections based on the ψ-scan of four strong reflections (minimum and maximum transmission factors 0.607 and 1.000). A total of 6263 reflections were measured, of which 5893 were unique and R_{int} = 0.017. A total of 4950 reflections with I > 3σ(I) were considered observed and used in the structural analysis. The centric space group was used on the basis of a statistical analysis of the intensity distribution and the successful refinement of the structure solved by Patterson methods and expanded by Fourier methods (PATTY^{15a}) and refinement by full-matrix least squares using the software package TeXsan^{15b} on a Silicon Graphics Indy computer. A crystallographic asymmetric unit consists of a univalent complex cation and a CF₃SO₃ anion. A total of 54 non-H atoms were refined anisotropically. A total of 23 H atoms at calculated positions with thermal parameters equal to 1.3 times that of the attached C atoms were not refined. Convergence for 488

(14) (a) van Houten, J.; Watts, R. J. *J. Am. Chem. Soc.* **1976**, *98*, 4853. (b) Parker, C. A.; Rees, W. T. *Analyst (London)* **1962**, *87*, 83. (c) Demas, J. N.; Crosby, G. A. *J. Phys. Chem.* **1971**, *75*, 991.

(15) (a) PATTY: Beurskens, P. T.; Admiraal, G.; Beurskens, G.; Bosman, W. P.; Garcia-Granda, S.; Gould, R. O.; Smits, J. M. M.; Smykalla, C., 1992. The DIRDIF program system, Technical Report of the Crystallography Laboratory, University of Nijmegen, Nijmegen, The Netherlands. (b) TeXsan: Crystal Structure Analysis Package, Molecular Structure Corp., 1985, 1992.

(13) (a) Gagne, R. R.; Koval, C. A.; Lisensky, G. C. *Inorg. Chem.* **1980**, *19*, 2854. (b) Che, C. M.; Wong, K. Y.; Anson, F. C. *J. Electroanal. Chem., Interfacial Electrochem.* **1987**, *226*, 211.

Table 2. Selected Bond Distances (Å) and Bond Angles (deg) for 6

Re(1)–S(1)	2.525(2)	Re(2)–S(1)	2.530(2)
Re(1)–N(2)	2.164(5)	Re(2)–N(4)	2.177(5)
Re(1)–N(1)	2.175(5)	Re(2)–N(3)	2.166(5)
Re(1)–C(1)	1.927(8)	Re(1)–C(2)	1.906(8)
Re(1)–C(3)	1.913(7)	Re(2)–C(21)	1.914(8)
Re(2)–C(22)	1.912(8)	Re(2)–C(23)	1.919(7)
Re(1)–S(1)–Re(2)	126.3(8)	Re(1)–S(1)–C(14)	112.3(2)
Re(2)–S(1)–C(14)	110.5(2)	N(1)–Re(1)–N(2)	74.4(2)
N(3)–Re(2)–N(4)	74.7(2)	S(1)–Re(1)–N(1)	82.4(1)
S(1)–Re(1)–N(2)	90.8(1)	S(1)–Re(2)–N(4)	80.6(1)
S(1)–Re(2)–N(3)	89.5(1)	S(1)–Re(1)–C(1)	94.6(6)
S(1)–Re(1)–C(2)	87.8(2)	S(1)–Re(1)–C(3)	174.8(2)
S(1)–Re(2)–C(21)	86.1(2)	S(1)–Re(2)–C(22)	95.4(2)
S(1)–Re(2)–C(23)	73.3(3)		

variable parameters by least-squares refinement on F with $w = 4F_o^2/\sigma^2(F_o^2)$, where $\sigma^2(F_o^2) = [\sigma^2(I) + (0.009 F_o^2)^2]$ for 4950 reflections with $I > 3\sigma(I)$, was reached at $R = 0.029$ and $wR = 0.039$ with a secondary extinction coefficient of $3.319 23 e^{-6}$ and goodness-of-fit of 1.74. $(\Delta/\sigma)_{\max} = 0.03$ for the complex cation. The final difference Fourier map was featureless, with maximum positive and negative peaks of 1.62 and $1.07 e \text{ \AA}^{-3}$, respectively. Crystal and structure determination data for **6** are summarized in Table 1. The final agreement factors for **6** are given in Table 1. Selected bond distances and angles are summarized in Table 2. The atomic coordinates and thermal parameters are given as supporting information.

Results and Discussion

Reaction of $[\text{Re}(\text{L}-\text{L})(\text{CO})_3(\text{MeCN})]\text{OTf}$ ($\text{L}-\text{L} = \text{phen}, \text{bpy}, \text{Me}_2\text{-bpy}$) with substituted thiophenol $\text{HSC}_6\text{H}_4\text{-X-}p$ ($\text{X} = \text{CH}_3, \text{OCH}_3, \text{C}(\text{CH}_3)_3, \text{Cl}, \text{F}$) in the presence of triethylamine in THF at room temperature under an inert atmosphere of nitrogen afforded the corresponding monomeric and dinuclear complexes. Separation of the products was achieved by column chromatography on silica gel using dichloromethane–acetone (9:1 v/v) as eluent. Subsequent recrystallization from slow evaporation of diethyl ether into acetone solution of the complexes gave crystals of $[\{\text{Re}(\text{L}-\text{L})(\text{CO})_3\}_2(\mu\text{-SC}_6\text{H}_4\text{-X-}p)]\text{OTf}$ [$\text{L}-\text{L} = \text{phen}, \text{X} = \text{CH}_3$ (**1**), OCH_3 (**2**), $\text{C}(\text{CH}_3)_3$ (**3**), Cl (**4**), F (**5**); $\text{L}-\text{L} = \text{bpy}, \text{X} = \text{CH}_3$ (**6**); $\text{L}-\text{L} = \text{Me}_2\text{-bpy}, \text{X} = \text{CH}_3$ (**7**)] in good yield. All the newly synthesized compounds gave satisfactory elemental analyses and have been characterized by ^1H NMR, IR, and positive FAB-MS. The crystal structure of complex **6** has also been determined.

Figure 1 shows the perspective drawing of the complex cation of **6** with atomic numbering scheme. The structure of the complex cation consists of two rhenium diimine moieties bridged by the thiolato ligand, $\mu\text{-SC}_6\text{H}_4\text{-CH}_3\text{-}p$, with a $\text{Re}(1)\text{-S}(1)\text{-Re}(2)$ bond angle of $126.32(8)^\circ$. The coordination geometry at each Re atom is distorted octahedral with the three carbonyl ligands arranged in a *facial* fashion. The $\text{S}(1)\text{-Re}(1)\text{-C}(3)$ and $\text{S}(1)\text{-Re}(2)\text{-C}(23)$ bond angles of $174.8(2)$ and $173.3(2)^\circ$ show a slight deviation from an ideal octahedral geometry. Although the Re-S σ -bonds are free to rotate, it is interesting to note that the planes of the two bipyridyl ligands and the phenyl ring of the bridging thiolato ligand show a stacked conformation, with dihedral angles between the idealized planes of the bipyridyl units and the phenyl ring of 14.57 and 14.58° . For the $\text{Re}(\text{I})$ metal centers, the $\text{N}(1)\text{-Re}(1)\text{-N}(2)$ [$74.4(2)^\circ$] and $\text{N}(3)\text{-Re}(2)\text{-N}(4)$ [$74.7(2)^\circ$] bond angles are substantially smaller than 90° as the result of the bite

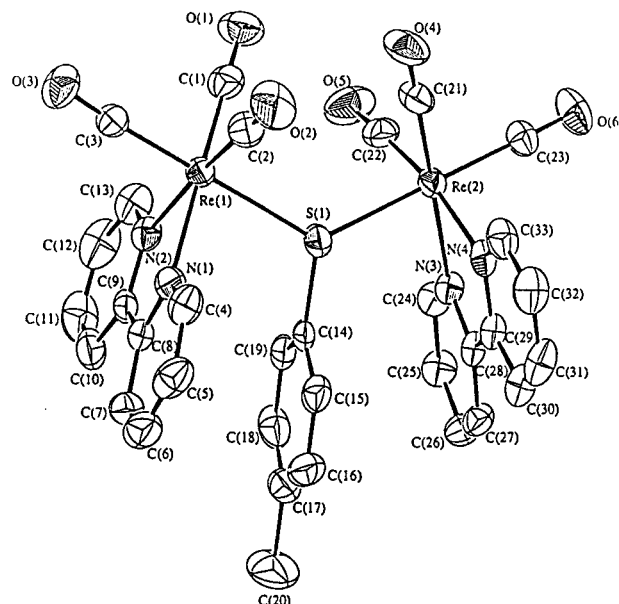


Figure 1. Perspective drawing of the complex cation of **6** with atomic numbering scheme. Thermal ellipsoids are shown at the 35% probability levels.

Table 3. Photophysical Data for Complexes 1–7

complexes	medium (TK)	$\lambda_{\text{em}}/\text{nm}$ ($\tau_o/\mu\text{s}$)	quantum yield, ^a Φ_{em}
1	solid (298)	563 (1.42)	0.012
	solid (77)	575	
	CH_2Cl_2 (298)	611 (0.11)	
2	solid (298)	564 (0.15, 0.81) ^b	0.010
	solid (77)	576	
	CH_2Cl_2 (298)	615 (0.11)	
3	solid (298)	575 (0.2)	0.011
	solid (77)	582	
	CH_2Cl_2 (298)	615 (0.10)	
4	solid (298)	562 (0.40)	0.015
	solid (77)	556	
	CH_2Cl_2 (298)	606 (0.14)	
5	solid (298)	547 (1.42)	0.012
	solid (77)	552	
	CH_2Cl_2 (298)	610 (0.14)	
6	solid (298)	581 (0.14)	0.002
	solid (77)	578	
	CH_2Cl_2 (298)	620 (0.14)	
7	solid (298)	550 (0.18)	0.020
	solid (77)	565	
	CH_2Cl_2 (298)	590 (0.15)	

^a Quantum yield was measured at room temperature using $[\text{Ru}(\text{bpy})_3]^{2+}$ as a standard. From ref 14. ^b Biexponential.

distances exerted by the steric requirements of each chelating bipyridyl ligand.^{5a-c} The average bond distances of Re-S [$2.527(7) \text{ \AA}$] and Re-C [$1.915(9) \text{ \AA}$] are found to be comparable to those observed in $[\text{Re}(\text{CO})_3\text{SR}]_4$.^{10c}

The electronic absorption spectra of complexes **1–7** show a high-energy absorption at $\sim 275 \text{ nm}$ and low-energy absorption shoulders at $\sim 430 \text{ nm}$ in CH_2Cl_2 . The low-energy absorption shoulders are likely to arise from a $d_{\pi}(\text{Re}) \rightarrow \pi^*(\alpha, \alpha'\text{-diimine})$ MLCT transition (Table 3), as similar assignments have been suggested in previous spectroscopic work on $\text{Re}(\text{I}) \alpha, \alpha'\text{-diimine}$ systems.^{1–5} Excitation of all the complexes in the solid state and in CH_2Cl_2 solution at $\lambda > 350 \text{ nm}$ at room temperature resulted in intense yellow-green luminescence. The photophysical data are summarized in Table 3. The emission energies are similar to those observed in other $\text{Re}(\text{I}) \alpha, \alpha'\text{-diimine}$ systems.^{1–5} The higher emission

Table 4. Excited State Parameters for Complexes 1–5^a

complex	$E_{em} \times 10^{-3}/\text{cm}^{-1}$	Φ_{em}	τ_0/ns	$k_r \times 10^{-3}/\text{s}^{-1}$	$k_{nr} \times 10^{-3}/\text{s}^{-1}$	$\ln k_{nr}$
1	16.37	0.012	110	109.09	8.98	16.01
2	16.26	0.010	110	90.91	9.00	16.01
3	16.26	0.011	100	110.00	9.89	16.11
4	16.50	0.015	140	107.14	7.04	15.77
5	16.50	0.012	140	85.71	7.06	15.77

^a k_{nr} is the radiationless decay rate, k_r is the radiative decay rate, Φ_{em} is the luminescent quantum yield, and E_{em} is the emission energy maximum.

energy in **7** compared to **6**, in accordance with the trend in MLCT absorption energies, is due to the higher π^* orbital energy of Me₂-bpy as a result of the electron-donating effect of the methyl groups on the bpy ligand. It is therefore suggested that the emissions of the complexes are associated with a metal-to-ligand charge transfer triplet excited state. Table 4 shows the excited state decay parameters for E_{em} , Φ_{em} , τ_0 , k_r , and k_{nr} measured in degassed dichloromethane solution for complexes **1–5**. The least-squares fit to the data of the plot of $\ln k_{nr}$ vs E_{em} for complexes **1–5** gave a slope of -10.20 e V^{-1} and an intercept of 35.56, which are close to that of -11.76 e V^{-1} and 40.21, respectively, in a related system of $[\text{Re}(\text{bpy})(\text{CO})_3\text{L}]^+$ reported by Caspar and Meyer.^{4a} The linearity of the plot shows that the emissions of the closely related complexes in solution more or less follow the energy gap law. The relative insensitivity of the solution emission energies to the nature of the thiolate ligands in complexes **1–5** may suggest a ³MLCT origin for the emission, although one could not exclude the possibility of a mixed MLCT/LLCT character, derived from a $p(\text{S}) \rightarrow \pi^*(\alpha, \alpha'$ -diimine) ligand-to-ligand charge transfer (LLCT) transition, in particular, in the solid state.

The cyclic voltammograms of complexes **1–7** in acetonitrile (0.1 mol dm⁻³ nBu₄NPF₆) display an irreversible and two quasi-reversible oxidation couples (+1.17 to +2.00 V vs SCE) and two quasi-reversible reduction couples (-1.21 to -1.55 V vs SCE). The cyclic voltammograms showing the oxidation and the reduction of complex **1** are shown in Figure 2a and b, respectively, and the electrochemical data are summarized in Table 5. The first reduction couple was tentatively assigned as an α, α' -diimine ligand-centered reduction,^{3b,6c,d} as it occurred at almost identical potential for complexes **1–5** with the same 1,10-phenanthroline ligand being involved. The more negative reduction potential observed in **7** relative to that in **6** is in accordance with the reduced ease of reduction of 5,5'-Me₂-bpy as a result of its higher π^* -orbital energy. The second reduction process may involve either a diimine-centered reduction or a metal-based Re(I) to Re(0) reduction as suggested in related systems.^{6c,d} Upon scanning to more negative potential (-2.0 to -2.5 V), two to five additional ill-defined irreversible reduction waves are observed. Such additional reduction waves have also been observed by scanning $[\text{Re}(\alpha, \alpha'$ -diimine)(CO)₃(MeCN)]⁺ to such negative potential. The peak current ratios for the first and third oxidation couples of 1.00–1.14 together with the ΔE_p values of slightly larger than that of the ferrocenium–ferrocene couple suggest the quasi-reversible nature of the couples. In view of the similarity in the peak current for the first oxidation couple to that for the reductions which are believed to be one-electron

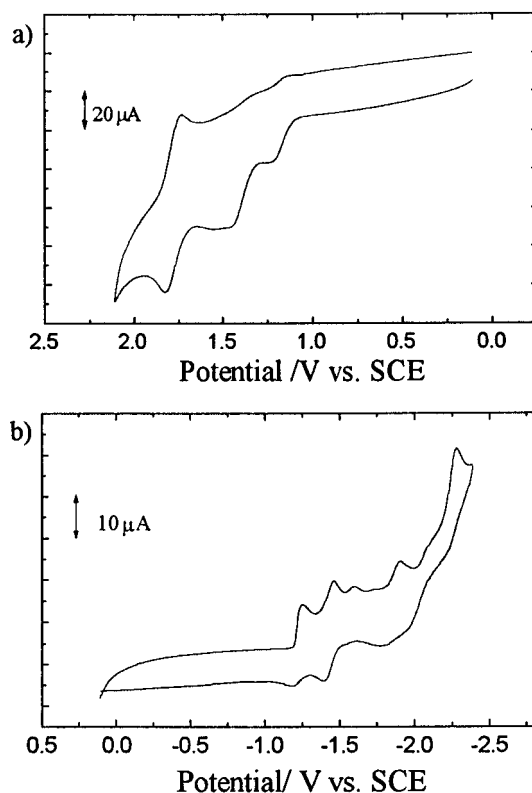


Figure 2. Cyclic voltammogram showing (a) the oxidation (scan rate, 100 mV s⁻¹) and (b) reduction (scan rate, 20 mV s⁻¹) of complex **1** in acetonitrile (0.1 mol dm⁻³ nBu₄NPF₆).

Table 5. Electrochemical Data for Complexes 1–7^a

complexes	$E_{1/2}^d/\text{V vs SCE}(\Delta E_p/\text{mV})$	
	reduction ^b	oxidation ^c
1	-1.21 (67)	+1.19 (66)
	-1.42 (67)	+1.46 ^e
2	-1.23 (68)	+1.17 (69)
	-1.43 (68)	+1.55 ^e
3	-1.22 (65)	+1.78 (68)
	-1.44 (68)	+2.00 ^e
4	-1.22 (65)	+1.18 (62)
	-1.44 (68)	+1.43 ^e
5	-1.21 (70)	+1.78 (58)
	-1.41 (63)	+1.78 (66)
6	-1.21 (69)	+1.24 (66)
	-1.40 (68)	+1.50 ^e
7	-1.21 (69)	+1.78 (66)
	-1.40 (68)	+1.22 (62)
6	-1.25 (72)	+1.47 ^e
	-1.43 (66)	+1.78 (63)
7	-1.25 (72)	+1.19 (69)
	-1.43 (66)	+1.43 ^e
7	-1.36 (64)	+1.78 (66)
	-1.55 (68)	+1.18 (66)
		+1.42 ^e
		+1.76 (69)

^a In acetonitrile (0.1 mol dm⁻³ NBu₄PF₆). Working electrode: glassy carbon; ΔE_p of Fc⁺/Fc ranges from 62 to 64 mV. ^b Scan rate, 100 mV s⁻¹. ^c Scan rate, 20 mV s⁻¹. ^d $E_{1/2} = (E_{pa} + E_{pc})/2$; E_{pa} and E_{pc} are peak anodic and peak cathodic potentials, respectively. ^e Peak anodic potential for the irreversible couple.

processes, the first oxidation couple was tentatively assigned as a Re(I) to Re(II) oxidation process. Similar oxidation waves have also been observed in related rhenium(I) α, α' -diimine systems.^{3a,b,4b,c,6} It is interesting to note that the third oxidation couple, following the second irreversible wave, appeared at almost identical potential for all the complexes. This, together with the

close resemblance of the potential value to those observed in $[\text{Re}(\text{phen})(\text{CO})_3(\text{MeCN})]^+$ and $[\text{Re}(\text{bpy})(\text{CO})_3(\text{MeCN})]^+$, suggested the generation of the respective $[\text{Re}(\text{L-L})(\text{CO})_3(\text{MeCN})]^+$ species. It is likely that the dinuclear rhenium complexes upon oxidation are unstable and decompose to give $[\text{Re}(\text{L-L})(\text{CO})_3(\text{MeCN})]^+$ with the loss of the thiolate ligand. A similar decomposition pathway has also been suggested in the related chlororhenium system.^{6d,e}

Preliminary work shows that a related $[\text{Re}(\text{L-L})(\text{CO})_3(\text{SC}_6\text{H}_4\text{-Cl-}p)]$ monomer that emits at ~ 720 nm can act as a metalloligand to form a heteroleptic dimer. Work is in progress to synthesize other monomers and

to explore their potential as precursors for heteroleptic dimers of rhenium(I).

Acknowledgment. V.W.-W.Y. acknowledges financial support from the Research Grants Council and The University of Hong Kong. K.M.-C.W. acknowledges the receipt of a Croucher Studentship administered by the Croucher Foundation.

Supporting Information Available: Tables giving fractional coordinates and thermal parameters, general displacement parameter expressions (U), and all bond distances and bond angles (13 pages). Ordering information is given on any current masthead page.

OM960797W